Acta Chemica Scandinavica A 39 (1985) 537–544

Crystal Structure and Properties of Ni_2SnP

SIGRID FURUSETH[a] and HELMER FJELLVÅG[b,*]

[a] Kjemisk institutt, Universitetet i Oslo, Blindern, N-0315 Oslo 3, Norway and
[b] Max Planck Institut für Festkörperforschung, D-7000 Stuttgart 80, BRD

The compound Ni_2SnP has been prepared directly from the elements and crystallized from tin melts. The structure has been determined from single crystal X-ray data (space group *Pnma*, unit cell dimensions a=1282.60(7), b=359.43(2), c=508.96(2) pm). The structure is related to the NiAs and MnP type structures, and is discussed in relation to the crystal structures of other NiX and NiY phases (X and Y being IV or V main group elements). The compound is a Pauli paramagnet and exhibits metallic conductivity.

The binary NiX (X=Si, Ge, Sn, Pb)[1–4] and NiY (Y=P, As, Sb, Bi)[5–8] phases with Ni/X (or Y) ≈ 1/1 adopt four different, but related structure types. Information is available for the structural and some physical properties of these phases,[1–10] but is practically lacking for the mixed systems NiX–NiY. As a part of the study of solid solution phases and ternary phases existing for NiX–NiY, results are presented for the phase Ni_2SnP.

EXPERIMENTAL

Preparation. Ni_2SnP was prepared by heating stoichiometric amounts of the elements (Ni: turnings from rods, 99.99 %; Johnson, Matthey Laboratories, Ltd., Sn: granules, 99.9 %; Fluka AG, P: lumps, 99.999 %; Koch-Light Laboratories, Ltd.) in evacuated, sealed silica tubes. After a first heat treatment at 1000 K for 1 week, the samples were crushed, reannealed at 900 K for 2 weeks, and cooled to room temperature over a period of 3 days.

Single crystals were prepared in tin melts (molar ratio Ni_2SnP:Sn ~ 1:5). The temperature of the melt was reduced from 900 to 300 K over a period of 2 weeks. Excess of tin was dissolved in hydrochloric acid, and needle-formed, grey single crystals, with bright metallic lustre were obtained (maximum crystal dimensions were 5.0×0.2×0.2 mm).

Characterization. The crystal symmetry and unit cell dimensions were obtained from single crystal Weissenberg data. Examination of the crystals by scanning electron microscopy with energy-dispersive X-ray analyzer gave a chemical composition $Ni_{2.2}SnP_{1.1}$, thus indicating the formula Ni_2SnP. This was later confirmed by the crystal structure determination. The homogeneity of the powder samples was ascertained from powder X-ray diffraction data [Guinier technique, Cu$K\alpha_1$-radiation (λ=154.059 pm) and Si (a=543.050 pm) as internal standard], and unit cell dimensions obtained by least-squares refinements. No significant deviation from stoichiometry (homogeneity range) was detected.

High- and low-temperature X-ray diffraction was performed on powdered samples between 100 and 1200 K in an Enraf-Nonius Guinier-Simon camera. X-ray powder data were handled by programs from Refs. 11 and 12. Magnetic susceptibility was measured by

* Present address: Institutt for Energiteknikk, N-2007 Kjeller, Norway.

0302-4377/85 $2.50

the conventional Faraday method between 80 and 1000 K (maximum field strength 8 kØ). DSC and DTA measurements were recorded between 100 and 1100 K with a Mettler TA 3000 system and a Mettler thermoanalyzer. Resistivity was measured between 4.2 and 300 K through four contact points on a single crystal.

Intensity data collection. A single crystal of dimensions 0.05×0.04×0.12 mm, needle axis [001], was chosen for the structure determination. Intensity data were recorded at room temperature with a Syntex $P\bar{1}$ autodiffractometer by the $\theta-2\theta$ scan technique using graphite monochromatized Mo$K\alpha$-radiation (λ=71.069 pm). Three standard reflections were used for scaling of the data. The standard reflections showed no significant fluctuations.

Intensity data were measured up to 2θ=65°. Of the 493 independent reflections the 409 having $I>3\sigma(I)$, were considered observed and were used in the refinement of the structural parameters.

Corrections were made for Lorentz and polarization effects, absorption, and isotropic extinction (an extinction parameter of $1.0\cdot10^{-4}$ was applied).

Form factors for neutral atoms and X-ray cross sections for absorption correction taken from Ref. 13 were applied in all calculations, using programs[14,15] for an ND 100/500 computer.

CRYSTAL DATA

Ni_2SnP, M=267.08.

Orthorhombic, space group *Pnma* nr. 62.

a=1282.60(7), b=359.43(2), c=508.96(2) pm, V=234.64(2)·10^6 pm^3, F(000)=484, Z=4

T=293 K, d_x=7.559 g cm^{-3}, μ(MoK_α)=266.0 cm^{-1}.

Magnetic susceptibility; Pauli paramagnet.

Electrical properties; metallic, $\rho=7.7\cdot10^{-5}$ Ohm cm at 293 K.

Thermal decomposition at 1005 K giving Ni_2P and Sn.

STRUCTURE DETERMINATION

The structure of Ni_2SnP was solved by combination of results from direct methods (MULTAN[15]) and the use of Patterson maps.

From the systematic absences, the space groups *Pnma* and *Pna*2_1 were possible, the space group *Pnma* was confirmed by the structure refinement.

From the Fourier map, the asymmetric unit was found to contain two nickel, one tin, and one phosphorous atom. Full matrix least squares refinement minimizing $\Sigma w(F_o-F_c)^2$, where $w=1/\sigma^2(F)$, using anisotropic temperature factors for all atoms, gave an R-value of 0.030 (R_w=0.034, S=1.51).

Atomic coordinates and equivalent isotropic thermal parameters are listed in Table 1. Lists of observed and calculated structure factors and anisotropic thermal parameters are available from the authors on request.

Table 1. Atomic coordinates and equivalent isotropic thermal parameters (A^2). Space group *Pnma*, 4 *c* positions. $B_{eq}=8\pi^2/3\sum_i\sum_j U_{ij}a_i^*a_j^*\mathbf{a}_i\mathbf{a}_j$.

Atom	x	y	z	B_{eq}
Ni1	0.1128(8)	1/4	0.5007(22)	0.427(2)
Ni2	0.4166(9)	3/4	0.5133(23)	0.597(2)
Sn	0.2925(4)	1/4	0.2800(12)	0.690(2)
p	0.0438(17)	3/4	0.2829(47)	0.457(3)

Table 2. Interatomic distances. Calculated standard deviations in parentheses.

Distance	(pm)	Distance	(pm)
Ni1–Sn(x1)	256.6(1)	Ni2–Sn(x2)	268.1(1)
Ni1–Sn(x2)	259.6(1)	Ni2–Sn(x1)	300.9(2)
Ni1–P(x2)	229.2(2)	Ni2–P(x1)	222.3(3)
Ni1–P(x1)	229.3(3)	Ni2–P(x2)	231.9(2)
Ni1–Ni2(x1)	250.9(2)	Sn–Sn(x2)	330.2(1)
Ni1–Ni2(x1)	263.7(2)	Sn–P(x2)	329.0(3)
Ni1–Ni1(x2)	341.1(2)	Sn–P(x2)	331.2(3)
Ni1–Ni2(x2)	280.1(2)	P–P(x2)	306.4(4)

Table 3. Bond angles. Calculated standard deviations in parentheses.

Angle	(°)	Angle	(°)
Ni2–Ni1–Ni2	163.1(1)	Ni1–Sn–Ni1	87.8(1)
Sn–Ni1–Sn	79.5(1)	Ni1–Sn–Ni1	131.4(1)
Sn–Ni1–Sn	87.8(1)	Ni1–Sn–Ni2	52.8(1)
Sn–Ni1–P	84.4(1)	Ni1–Sn–Ni2	59.9(1)
Sn–Ni1–P	97.8(1)	Ni1–Sn–Ni2	99.8(1)
Sn–Ni1–P	98.5(1)	Ni1–Sn–Ni2	109.9(1)
P–Ni1–P	83.9(1)	Ni1–Sn–Ni2	115.4(1)
P–Ni2–P	103.5(1)	Ni2–Sn–Ni2	84.3(1)
		Ni2–Sn–Ni2	136.9(1)
Ni1–Ni2–Ni1	163.1(1)	Ni1–P–Ni1	103.5(1)
Ni2–Ni2–Ni2	79.9(1)	Ni1–P–Ni1	96.1(1)
Sn–Ni2–Sn	70.7(1)	Ni1–P–Ni2	71.4(1)
Sn–Ni2–Sn	84.3(1)	Ni1–P–Ni2	65.9(1)
Sn–Ni2–P	82.6(1)	Ni1–P–Ni2	118.5(1)
Sn–Ni2–P	85.9(1)	Ni1–P–Ni2	127.8(1)
Sn–Ni2–P	97.9(1)	Ni1–P–Ni2	144.1(1)
P–Ni2–P	101.8(1)	Ni2–P–Ni2	76.1(1)
P–Ni2–P	103.9(1)	Ni2–P–Ni2	101.8(1)

RESULTS AND DISCUSSION

The crystal structure of Ni_2SnP is shown in Fig. 1. Interatomic distances shorter than 350 pm are listed in Table 2, and some bond angles in Table 3.

The phosphorus atoms form bonds of normal length (222.3–231.9 pm) to 6 nickel atoms situated at the corners of a trigonal prism.

The tin atoms are coordinated to 5 nickel atoms at normal bonding distances (256.6–268.1 pm). Taking one additional Ni2 atom 300.9 pm away into account, the coordination polyhedron can be looked upon as a heavily distorted trigonal prism.

The Ni1 atoms are surrounded by 3 phosphorus and 3 tin atoms forming a fairly regular octahedron. In addition, two close Ni2 atoms (interatomic distances 250.9 and 263.7 pm) give rise to zig-zag Ni–Ni chains along [001].

The coordination polyhedron of the Ni2 atoms is less regular – 3 phosphorus and 2 tin atoms form together with a third tin atom 300.9 pm away a distorted octahedron. In addition

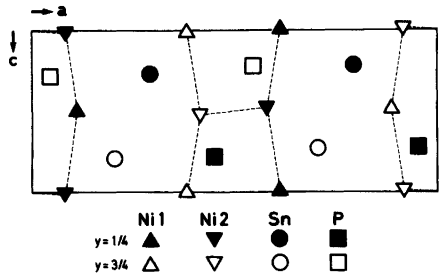

Fig. 1. Projection of the structure of Ni_2SnP on the *ac*-plane. Probable Ni–Ni bonding interactions are indicated by dotted lines.

to the 2 Ni1 atoms of the zig-zag chain along [001], two Ni2 atoms are also situated at distances (280.1 pm) suggesting bonding interactions, see Fig. 1.

The coordination octahedra of the Ni1 and Ni2 atoms share one side, forming chains along [001]. The chains are connected to neighbouring chains by common edges. The strong bonding in the [001] direction is reflected in the crystal form; needles with [001] as needle axis.

Ni_2SnP may formally by considered as a member of a possible ternary (solid solution) series $NiSn_xP_{1-x}$ with $x=0.5$. However, as stated earlier, no appreciable homogeneity range was found around the composition Ni_2SnP. Indeed the crystal structure of Ni_2SnP manifests an ordering of P and Sn, and the crystal structure hence differs from those adopted by the binary phases NiP and NiSn. It seems pertinent to discuss the crystal structure of Ni_2SnP in relation to the available data for other Ni*X* and Ni*Y* phases (*X*, *Y* being IV or V main group elements respectively.)

The 3*d*-element pnictides (*TY*) commonly crystallize with the NiAs or MnP type structures, and the MnP type is preferred when *Y* is of "small" size, *e.g.* P and As. NiP breaks this pattern by adopting its own structure type. The similar *TX* phases with *X*=Si,

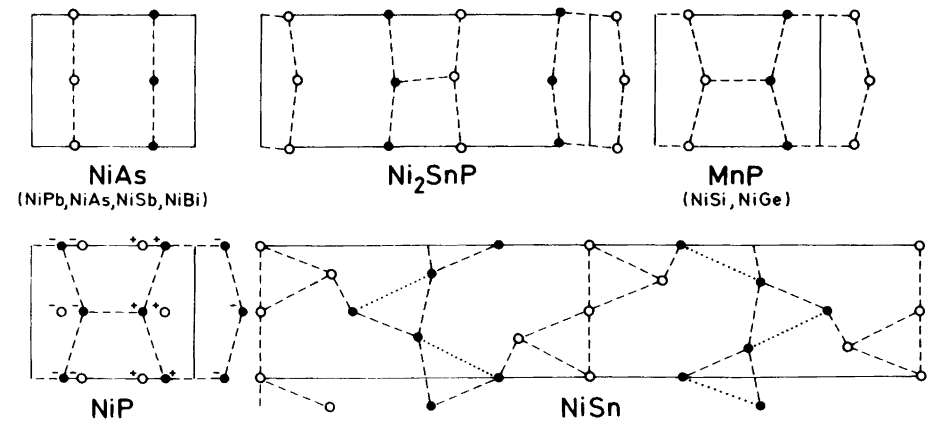

Fig. 2. Selected projections of some structure types showing one-, two- or three dimensional nets of metal-metal interactions. Non-metal atoms are omitted. (The NiAs, in orthohexagonal setting, MnP, and Ni_2SnP type structures are projected on the *ac*-plane, while the NiP and NiSn structures are projected on the *ab*-plane.) Metal-metal bonds are indicated by dotted lines. For NiP, + and − signs respectively, mean below and above the plane of projection. Open and filled symbols refer to planes separated by half the length of the projection axis.

Table 4. Structure types adopted by different Ni$X(Y)$ phases X,Y being a IV or V main group element, respectively. The number of short metal-metal distances per metal atom and their lengths are included. (The shortest Ni–Ni distance not tabulated is d(Ni–Ni)=321 pm for NiSn.)

Phase	Structure type	Number of short Ni–Ni contacts and distances	Ref.
NiSi	MnP	2 (268.4 pm)+2 (268.8 pm)	1
NiGe	MnP	2 (277.9 pm)+2 (279.6 pm)	2
NiSn[a]	NiSn	Ni(1), Ni(2), Ni(4): 4 Ni–Ni contacts Ni(3), Ni(5) : 3 Ni–Ni contacts	3
NiPb	NiAs	2 (264.0 pm)	4
NiP	NiP	2 (253.2 pm)+1 (275.6 pm)	5
NiAs	NiAs	2 (255.0 pm)	6
NiSb	NiAs	2 (256.9 pm)	7
NiBi[b]	NiAs	2 (267.2 pm)	8

[a] Ni(1) 2×260.0 pm+2×282.7 pm; Ni(2) 2×260.0 pm+2×303.0 pm; Ni(3) 2×261.1 pm+1×281.5 pm; Ni(4) 2×267.0 pm+1×282.7 pm+1×303.0 pm; Ni(5) 2×267.1 pm+1×281.5 pm. [b] Superstructure is present.[16]

Ge, Sn or Pb also show diversity with respect to crystal structure. NiSi and NiGe adopt the MnP type, NiPb the NiAs type, while NiSn adopts its own structure type. Since NiP and NiSn both are outstanding with respect to crystal structure, the discussion of the structure of Ni_2SnP will comprise the above mentioned structure types. The structure types adopted by Ni$X(Y)$ phases are given in Table 4, and selected projections are shown in Fig. 2. In all cases the metal atoms exhibit (slightly distorted) octahedral coordination to the non-metal atoms (X,Y). Non-metal atoms are for the aspect of clarity omitted from the figure. A common feature of the group of NiX and NiY phases is short Ni–Ni distances, *cf.* Table 4 (for a comparison, the Ni–Ni distance in metallic Ni is 248 pm). The different ways these probably bonding interactions are met for the structure types adopted by the NiX and NiY phases are shown in Fig. 2. The complexity of the nets formed by the Ni–Ni "bonds" increase from the NiAs type (linear chains) via NiP and Ni_2SnP (two dimensional slabs) to the MnP and NiSn types (three-dimensional network.)

When considering the topology of the metal-metal bonds in Ni_2SnP, the resemblance to the NiAs and MnP types is demonstrated through the projections of the different structure types in Fig. 2. The characteristic, inter-penetrating zig-zag chains of metal-metal "bonds" (*viz.* short distances believed to reflect bonding interactions) in the MnP type are only partly retained in the Ni_2SnP type structure. In Ni_2SnP the Ni–Ni "bonds" build two-dimensional nets separated by the large Sn-atoms.

A comparison of the metal sublattices in Ni_2SnP and NiP type structures is also included in Fig. 2. In NiP each Ni atom has 3 close neighbours while in Ni_2SnP the Ni atoms have alternating 2 and 4 neighbours (on the average also 3, *cf.* Tables 2,4). It is interesting to note that the average Ni–P bond distances are almost identical for NiP and Ni_2SnP (228.8 and 228.9 pm, respectively), and that the same is true for the Ni–Sn bond distances in NiSn and Ni_2SnP (262.4 and 261.3 pm).

A rather common feature for the orthorhombic MnP type phases (especially *T*As binary and ternary phases) is the high-temperature second order phase transition to the hexagonal NiAs-type structure. In order to elucidate whether Ni_2SnP shows similar behaviour, high

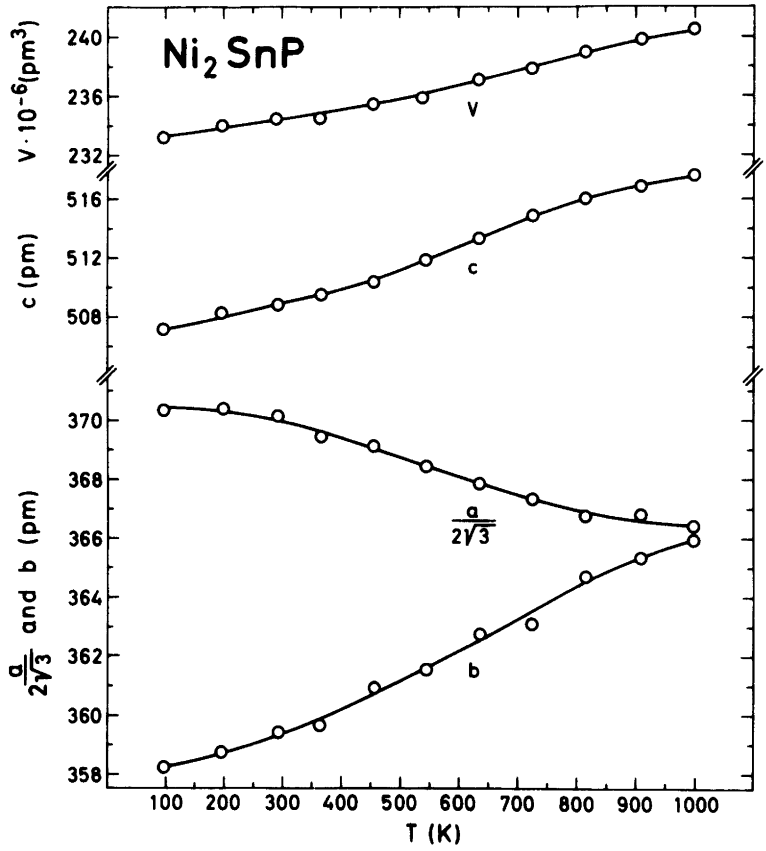

Fig. 3. Temperature dependence of the unit cell dimensions of Ni_2SnP between 100 and 1000 K.

temperature X-ray diffraction experiments were carried out. The results obtained are presented in Fig. 3.

The MnP type structure is related through the relations $\bar{c}_{MnP}=2\bar{a}_{NiAs}+\bar{b}_{NiAs}$, $\bar{b}_{MnP}=\bar{b}_{NiAs}$, $\bar{a}_{MnP}=\bar{c}_{NiAs}$ to the NiAs type. Thus in the orthohexagonal limit $(c/b)_{MnP}=\sqrt{3}$ (the orthorhombic distortion usually introduces an axial ratio $(c/b)_{MnP}>\sqrt{3}$), see *e.g.* Refs. 17,18. For Ni_2SnP corresponding considerations give $a=2a_{NiAs}\cdot\sqrt{3}$, $b=b_{NiAs}$ and $c=c_{NiAs}$. At 100 K $a/2b=1.791$, which is considerably larger than $\sqrt{3}$. At higher temperatures this axial ratio is reduced (*cf.* Fig. 3) in agreement with the expectations for transformation towards a hexagonal structure. At 1000 K $a/2b=\sqrt{3}$ within the estimated errors, however, above this temperature Ni_2SnP decomposes thermally. An axial ratio of $\sqrt{3}$ is of course only a necessary and not a sufficient requirement for this type of a continuous phase transition (which in the case of the NiAs type structure requires a randomization of P and Sn). The integrated intensities of the Bragg reflections were used in order to get information on any change in positional parameters. However, the results confirmed that the orthorhombic Ni_2SnP type structure is retained up to 1000 K. Of the thermal expansion curves in Fig. 3, the one for *a* shows an unexpected contraction with increasing temperature. An implication of this, assuming the same positional parameters for Ni2 at 1000 K as at 293

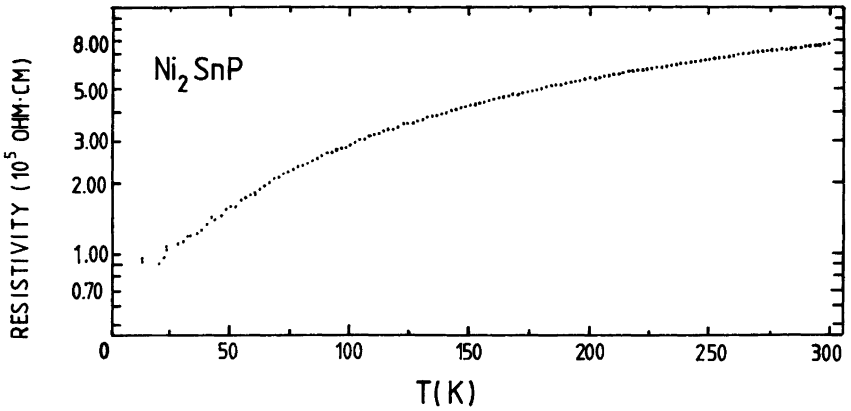

Fig. 4. Resistivity *vs.* temperature for Ni_2SnP between 12 and 300 K.

K (*cf.* Table 1), is an unchanged length for the Ni2–Ni2 "bond" (*viz.* 280.0 pm at 1000 K). This supports the picture of some bonding interactions between the Ni-atoms.

One might expect that the relatively large differences in crystal structure for the Ni*X* and Ni*Y* phases are reflected in variation of the magnetic, electrical and optical properties. Unfortunately no complete sets of such information are at present available, but the properties seem to be only slightly influenced by variation in crystal structure.

Data for the resistivity of Ni_2SnP were obtained for temperatures between 4.2 and 300 K (see Fig. 4), and Ni_2SnP shows metallic behaviour throughout this temperature range. This finding complies well with corresponding results for NiSb[19] and NiBi[20] (superconductor below 4.25 K).

The measured magnetic susceptibility for Ni_2SnP shows slight diamagnetic ($\chi_g = -2 \cdot 10^{-7}$ e.m.u./g at 293 K) behaviour for $T < \sim 700$ K, and slightly paramagnetic ($\chi_g = 1.4 \cdot 10^{-7}$ e.m.u./g at 950 K) for 700 K $< T <$ 1000 K. However, after diamagnetic corrections due to core electrons, Ni_2SnP is to be classified as a Pauli paramagnet over the entire temperature interval. The magnetic susceptibility increases slightly with temperature. These findings comply well with the reported paramagnetic properties of NiSb[19], while for NiAs[21] the opposite temperature dependence of the magnetic susceptibility was found.

Acknowledgements. The authors want to thank Dr. Bauhofer (Max-Planck Institut für Festkörperforschung, Stuttgart) for performing the measurements of electric properties, and B. Klewe (University of Oslo) for help and advice concerning the single crystal X-ray measurements.

REFERENCES

1. Toman, K. *Acta Crystallogr. 4* (1951) 462.
2. Pfisterer, H. and Schubert, K. *Z. Metallk. 41* (1950) 358.
3. Bhargava, M.K. and Schubert, K. *J. Less-Common Met. 33* (1973) 181.
4. Bitti, R.R., Dixmier, J. and Guinier, A. *C.R. Acad. Sci. (Paris) Ser. B 266* (1968) 565.
5. Larsson, E. *Arkiv Kemi 23* (1964) 335.
6. Heyding, R.D. and Calvert, L.D. *Can. J. Chem. 35* (1957) 449, 1205.
7. Kjekshus, A. and Walseth, K. *Acta Chem. Scand. 23* (1969) 2621.
8. Hägg, G. and Funke, G. *Z. Phys. Chem. Abt. B 6* (1929) 272.

9. Kjekshus, A. and Pearson, W.B. *Progr. Solid State Chem. 1* (1964) 83.
10. Ellner, M. *J. Less-Common Met. 48* (1976) 21.
11. Malmros, G. and Werner, P.-E. *Acta Chem. Scand. 27* (1973) 493.
12. Ersson, N.O. *Program CELLKANT* Kemiska institutionen, Uppsala Universitet, Uppsala, Sweden.
13. *International Tables for X-Ray Crystallography,* Kynoch Press, Birmingham 1977, Vol. 4.
14. Groth, P. *Acta Chem. Scand. 27* (1973) 3131.
15. Germain, G., Main, P. and Woolfson, M.M. *Acta Crystallogr. A 27* (1971) 368.
16. Fjellvåg, H. *Unpublished results.*
17. Selte, K. and Kjekshus, A. *Acta Chem. Scand. 27* (1973) 3195.
18. Endresen, K., Furuseth, S., Selte, K., Kjekshus, A., Rakke, T. and Andresen, A.F. *Acta Chem. Scand. A 31* (1977) 249.
19. Chen, T., Rogowski, D. and White, R.M. *J. Appl. Phys. 49* (1978) 1425.
20. Alekseevskii, N.E., Brandt, N.B. and Kostina, T.I. *Izv. Akad. Nauk SSSR. 16* (1952) 223.
21. Fjellvåg, H., Selte, K. and Stave, F.E. *Acta Chem. Scand. A 38* (1984) 687.

Received March 29, 1985.